High level strategy for revisiting objects with low cost AUVs

Thibaut NICO
ENSTA Bretagne / Lab-STICC
ECA Group
Brest, France
thibaut.nico@ensta-bretagne.org

Luc JAULIN
ENSTA Bretagne / Lab-STICC
Brest, France
luc.jaulin@gmail.com

Benoit ZERR
ENSTA Bretagne / Lab-STICC
Brest, France
benoit.zerr@ensta-bretagne.fr

Sébastien TAUVRY
ECA Group
Brest, France
tauvry.s@ecagroup.com

Hervé OTT
ECA Group
Toulon, France
ott.h@ecagroup.com

***Abstract*—This paper describes a high level strategy to guarantee the revisit of a target in underwater environment by an Autonomous Underwater Vehicle (AUV) subject to high drift in position and equipped with specific exteroceptive sensors such as sonars or cameras. It assumes the availability of a certain *a priori* map of the environment. Firstly, based on the Field Of View (FOV) of the exteroceptive sensor and the characteristics of the different landmarks in the map, a registration map is computed. This indicates the sets of the robot configurations able to detect the different landmark considered. All these sets called relocation areas enable to relocate the robot position and reduce its uncertainty by detecting the geolocalized landmarks. These relocation areas are the nodes of a hyper-graph. Between two nodes, the vehicle navigates by dead-reckoning. Based on the backward reach set of a registration map, the links between the different registration maps can be created according to a motion model taking into account uncertainties. Finally, a backward graph search minimizes a cost function to propose a strategy of revisit of intermediate landmarks to connect the starting position and the relocation area(s) of the target you would like to revisit.**

***Index Terms*—motion planning, uncertainties, guarantee, set-membership, interval analysis, graph search, AUV, sonar**

I. Introduction

Revisiting previously located targets in underwater environment may be of great interest in many and various domains. Indeed, some Features Of Interest (FOI) may be revealed during a survey mission conducted usually by a surface vessel or an Autonomous Underwater Vehicle (AUV) equipped with ranging and imaging sonar to map the seabed. The FOI could be an old wreck in archaeological scientific missions [1] that would be interesting to investigate more with cameras [2] to determine the origin and the age of the vessel for example. In Mine CounterMeasure (MCM) missions [3], it is vital to identify and neutralize some potential dangerous objects called mines to secure a naval transit or to invade an enemy harbour. This task, usually performed by human divers, is intended to be replaced by autonomous robot to avoid any human loss. Due to the self detonation of the robot for mine clearance, the design of the robot is aimed to be low cost.

Revisiting a previously mapped object, called a target, in underwater environment with a low cost AUV is a challenging task due to the lack of absolute positioning system (GPS). Acoustic beacons navigation [4] may provide accurate localization but requires setting up some beacons in the search area and has limited range. Navigation based on Inertial Navigation System (INS) generally coupled with a Doppler Velocity Log (DVL) has been widely used in subsea operations but are too expensive for the low cost design. If an *a priori* map of the environment is available, an alternative navigation solution is possible even for long range mission. This map may contain some reference points called landmarks such as man-made objects, rocks or sand-ripples regions for example and a FOI such as a mine called the target. The landmarks and the target may have been detected by an automatic algorithm or manually by an operator in the sonar images of a previously survey mission. Based only on an exteroceptive sensor such as a Forward Looking Sonar (FLS) and a compass for the heading measurement, renavigating directly this environment with this low cost AUV does not guarantee the revisit of the desired target. Indeed, it requires heavy data association algorithms [5] to match the relative map to the reference map to self locating relatively to the desired target. Moreover, it requires a diving position near a landmark field to perform the multi-hypotheses data association. In [6] a navigation based on a video mosaic previously computed with a sequence of camera images is proposed. The position of the robot is estimated by registering the current image to the mosaic and then it is able to correct the displacement from the defined path. However, the use of an optical camera requires a minimum of visibility and to navigate close to the seabed.

A path finding strategy is then proposed in this article to provide a strategy for the revisit of the FOI based on these geolocalized landmarks.

Path planning [7] [8] has been the topic of many researches in any kind of environment. Nevertheless when a robot operates in a real world and Global Positioning System (GPS) denied environment such as the underwater environment, it is subject to drift since it relies on odometric techniques to estimate its configuration, making mission objectives very difficult to complete. When the robot has a reliable navigation, a simple path planning algorithm, providing a nominal path, can be proposed [9]. However, due to the low cost design,

978-1-7281-1450-7/19/$31.00 ©2019 IEEE

a such planned path cannot be followed correctly since the error in position increases rapidly. To overcome this issue, the uncertainties have to be taken into account at the planning phase.

Path planning with uncertainty was mainly interested in extending the methods that do not consider uncertainty. Some are focused only on the feasibility of the path with the uncertainty propagation to avoid obstacles, but in this article the focus is on the concept of landmark relocation to reduce the uncertainty accumulated during the navigation since an *a priori* map is available. The notion of registration maps based on an exteroceptive sensor has been introduced by the Sensory Uncertainty Fields (SUF) in [10]. It indicates in the state space represented by a grid the relocation ability of an exterceptive measurement at each pose in the grid but the path planner didn't take into account the propagation of the uncertainty along the path. It only provides a path that uses the exterceptive sensor at the best. This notion has been proposed in [11] as "coastal navigation" to make the analogy to ships navigation when GPS is not available. The concept of relocation areas has already been studied in [12] where "disk" relocation areas are considered. If the robot enters one of these zones, its uncertainty is reset to zero or a small value and remains constant in this zone. The planner is then based on the notion of preimages backchaining [13] to find a motion strategy despite the uncertain heading in the case of a holonomic system. In [14], they propose a motion strategy composed of sensor-based motion commands in a polygonal obstacles environment that guarantee the reachability of the walls and the relocation areas defined with a potential field method. The notion of relocation region has been defined as "detection region" in [15] where a discrete environment space in the form of a grid is considered. The uncertainty of the robot along the path is propagated in the augmented pose-uncertainty space [16]. However, even if the step size is strongly reduced, the planner will spend most of time outside the relocation areas. In [17] [18] [19], a sampling motion planner called roadmaps is proposed [20] where the propagation of the uncertainty along Dubins paths [21] is used to take into account non-holonomic constraint. The relocation process is only active when the uncertainty accumulated can be reduced. To overcome the non-holonomic issue, a sampling based algorithm called Rapidly-exploring Random Tree (RRT) is effecient. It has even been extended to set-membership approach to propose a robust path in [22]. However the concept of relocation is only based on the more likely position (mean position) [23] by making sensor simulation [24] around this position. It provides a "nominal path" as in [19] and assumes the mean of the system is fully controllable, that means the controller is always able to drive the state estimate on the desired path as in the other sampling algorithm with uncertainty propagation called Belief Road Map (BRM) [25].

The solution adopted in the paper is the use of a registration map computed according to the visibility area of the exteroceptive sensor and then a motion planner inspired by the work in [12] on the preimages backchaining of some relocation areas.

This paper is organised as follows. Firstly the problem statement is proposed. Next the concept of registration maps is proposed based on a set membership method via interval analysis. In Section IV the motion planner under uncertainty is presented based on the backprojection of the registration maps to create the edges in the graph construction. Finally Section V develops an experiment of the motion planner to guarantee the revisit of a target in underwater context based on simulation.

II. Problem statement

The problem of the motion planning proposed in this article consists in finding a sequence of open-loop strategies μ_i to join a goal region despite the uncertainties on the motion. This goal region corresponds to the robot poses that are able to detect the target (FOI) and is defined by the registration map associated to this target. The high-level open-loop plan π can then be expressed as follows:

$$\pi = (\mu_1, \mu_2, ..., \mu_k) \tag{1}$$

which is a sequence of k motion commands. These motion commands may refer to high-level strategies such as "Go to the North", "Follow the contour of a sand ripples region" or "Visually guide the robot to a defined position". These motion commands depend on exteroceptive measurements such as sonars or compass.

It is assumed that the robot is equipped by a compass that provides the heading information. However, this latter is not accurate and it will be assumed that it lays in a bounded interval to propose a set-membership approach of the motion planning contrary to probabilistic approaches [26]. It will then be assumed that the vehicle is able to follow an uncertain heading as in [12]. Moreover, the commands "Visually guide the robot to a defined position" or "Follow the contour of a sand ripples region" correspond to visually guided navigation [27] based on the images collected by a camera or a sonar and a detection algorithm. It is then assumed that a low-level controller exists and is able to perform these tasks. The open-loop plan is actually composed of closed-loop motion commands.

In this article, the focus will be on the directions (headings) to follow to navigate between the registration maps despite the presence of uncertainty in the direction to follow. The global plan π is then composed of alternated phases of reachability of a landmark and relocation process to join the departure area to reach the next landmark. This second phase corresponds to visually guided motion and is not treated here. The directions to follow are based on the backprojection of a registration map associated to a landmark. It will then be defined the omnidirectional and directional backprojections of a set according to the uncertainty on the direction coming from the compass measurements.

For simplicity reasons, only a 2D environment is considered. This assumption may be envisaged when the robot navigate at a constant altitude above the seabed. The landmarks are then only subsets of $\mathbb{R}^2$. It will be assumed that the landmarks in

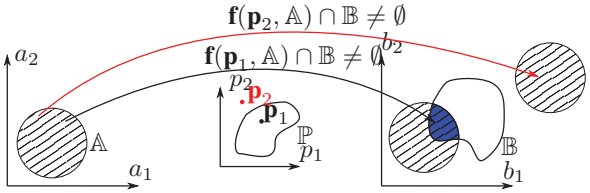

Fig. 1: Registration map concept. $\mathbb{P}$ is the set of parameter $\mathbf{p}$ of the function $\mathbf{f}$ such that after the transformation of the set $\mathbb{A}$ by $\mathbf{f}$, it intersects $\mathbb{B}$. A parameter vector $\mathbf{p}_2$ outside the solution set does not enable the intersection between $\mathbb{B}$ and the set $\mathbb{A}$ after transformation.

the map are detectable by the sonar or the camera embedded in the robot. Moreover the map is static and it assumes no change in the map. Moreovoer, it will be assumed indistinguishable landmarks meaning that the robot cannot make the difference between the different landmarks. The idea is to provide a strategy only based on the *a priori* landmarks present in the map. Now the concept of registration maps has to be firstly defined since it provides the set of robot poses able to relocate the robot position with respect to the geolocalized landmarks.

III. Registration maps

The registration map problem aims at finding the set $\mathbb{P}$ that corresponds to the robot configurations able to detect a part or entirely a landmark $\mathbb{B}$ based on the visibility area $\mathbb{A}$ of the sensor. It consists then in finding the parameters vector $\mathbf{p} \in \mathbb{P}$ of a possibly non linear transformation $\mathbf{f}$ such that $\mathbf{f}(\mathbf{p}, \mathbb{A}) \cap \mathbb{B} \neq \emptyset$ as depicted in Figure 1. $\mathbf{p}_1$ belongs to the set $\mathbb{P}$ meaning that after transformation by $\mathbf{f}$, the visibility area $\mathbb{A}$ intersects $\mathbb{B}$ represented by the blue area. On the contrary, $\mathbf{p}_2$ does not belong to $\mathbb{P}$ which leads to an empty intersection between $\mathbb{B}$ and the transformed set $\mathbf{f}(\mathbf{p}_2, \mathbb{A})$. This is defined as the map registration constraint. The function $\mathbf{f}$ may correspond to a translation, a rotation or the composition of both for example. This constraint is justified by the fact that detecting an element of a landmark enables to relocate the robot with respect to this landmark. The set $\mathbb{B}$ may be reduced to a singleton which is called a punctual landmark.

A. Visibility area of the sensor

The embedded exteroceptive sensor has a limited FOV such as sonars or cameras. It is assumed a patch exploration [28] meaning that the visibility area is not reduced to a singleton or a line sweep. This can be represented as a constraint. The visibility area is defined as the sensor field of view in [29]. Due to the assumption of a 2D environment, the visibility area is then also a subset of $\mathbb{R}^2$. The visibility area $\mathbb{V}$ at a defined robot position $\mathbf{x}$ can be defined as follows:

$$\mathbb{V}(\mathbf{x}) = \{\mathbf{z} \in \mathbb{R}^2 | \varphi(\mathbf{z}, \mathbf{x}) \leqslant 0\} \quad (2)$$

where $\varphi : \mathbb{R}^2 \times \mathbb{R}^3 \rightarrow \mathbb{R}$ is the visibility function which is assumed to be continuous.

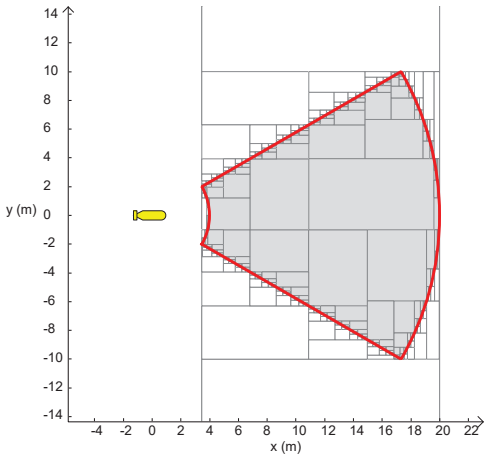

Fig. 2: Visibility area of a FLS at the pose defined by the yellow AUV. The light gray boxes are inside the set, the white boxes outside and the dark gray ones no conlusion can be made. Red pie is the enclosure of the solution set.

In this article, under the assumption of a forward looking sensor such as FLS (Forward Looking Sonar), the visibility area can be defined as follows:

$$\mathbb{V}(\mathbf{x}) = \{\mathbf{z} \in \mathbb{R}^2 | \sqrt{(z_1 - x_1)^2 + (z_2 - x_2)^2} \in [R_{min}, R_{max}] \\ \textbf{and } \operatorname{atan2}(z_2 - x_2, z_1 - x_1) - x_3 \in [-\theta_3, \theta_3]\} \quad (3)$$

where $\mathbf{x} = (x_1, x_2, x_3) = (x, y, \theta)$ is the pose of the robot, θ_3 is the half aperture angle and R_{min} (R_{max}) is the minimal (maximal) range of the sensor. The whole aperture angle is then $2\theta_3$.

A separator [30] can be built to provide an inner and an outer approximation of the set $\mathbb{V}(\mathbf{x})$ at a defined pose $\mathbf{x}$ using a paver, called SIVIA (Set Inversion Via Interval Analysis) [31], based on interval analysis [32]. This set is represented at the particular pose $\mathbf{x} = (0, 0, 0^\circ)$ in Figure 2 using a polar separator [33] for a range of detection between 4 and $20m$, and an half aperture angle $\theta_3 = 20^\circ$.

B. Registration map computation

Registration usually refers to image registration [34] or points cloud registration [35]. It has been applied to the underwater environment in [36] but here the registration map indicates the robot poses that are able to detect a considered landmark. It provides the robot poses that enable to relocate the robot position with respect to the geolocalized landmark.

The registration map problem is formulated as a set projection. Consider a function:

$$\mathbf{f} : \begin{cases} \mathbb{R}^2 \times \mathbb{R}^p & \rightarrow & \mathbb{R}^2 \\ (\mathbf{a}, \mathbf{p}) & \rightarrow & \mathbf{f}(\mathbf{a}, \mathbf{p}) \end{cases} \quad (4)$$

With $\mathbf{p} \in \mathbb{R}^P$, $\mathbb{A} \subset \mathbb{R}^2$, $\mathbb{B} \subset \mathbb{R}^2$ and $\mathbb{Z} \subset \mathbb{R}^2 \times \mathbb{R}^p$, the following notations are used:

$$\mathbf{f}(\mathbb{A}, \mathbf{p}) = \{\mathbf{b} | \exists \mathbf{a} \in \mathbb{A}, \mathbf{b} = \mathbf{f}(\mathbf{a}, \mathbf{p})\} \quad (5)$$

$$\mathbf{f}^{-1}(\mathbb{B}) = \{\mathbf{z} = (\mathbf{a}, \mathbf{p}) | \exists \mathbf{b} \in \mathbb{B}, \mathbf{b} = \mathbf{f}(\mathbf{a}, \mathbf{p})\} \quad (6)$$

$$proj_{\mathbf{p}}(\mathbb{Z}) = \{\mathbf{p} | \exists \mathbf{a}, (\mathbf{a}, \mathbf{p}) \in \mathbb{Z}\} \quad (7)$$

where the operator $proj()$ has been introduced in [37].

By considering the set:

$$\mathbb{P} = \{\mathbf{p} \in \mathbb{R}^p | \mathbf{f}(\mathbb{A}, \mathbf{p}) \cap \mathbb{B} \neq \emptyset\} \quad (8)$$

where $\mathbb{A}$ is the visibility area of the sensor at the particular pose $\mathbf{x} = (0, 0, 0°)$ and $\mathbb{B} \subset \mathbb{R}^2$ is the landmark.

A transformation vector $\mathbf{p}$ is consistent if after the transformation of $\mathbb{A}$, it intersects the set $\mathbb{B}$. This leads to:

$$\mathbf{f}(\mathbb{A}, \mathbf{p}) \cap \mathbb{B} \neq \emptyset \quad (9)$$

$$\Leftrightarrow \quad \exists \mathbf{a} \in \mathbb{A}, \mathbf{f}(\mathbf{a}, \mathbf{p}) \in \mathbb{B} \quad (10)$$

$$\Leftrightarrow \quad \exists \mathbf{a} \in \mathbb{A}, (\mathbf{a}, \mathbf{p}) \in \mathbf{f}^{-1}(\mathbb{B}) \quad (11)$$

$$\Leftrightarrow \exists \mathbf{a}, (\mathbf{a}, \mathbf{p}) \in \mathbb{R}^2 \times \mathbb{R}^p \wedge (\mathbf{a}, \mathbf{p}) \in \mathbf{f}^{-1}(\mathbb{B}) \quad (12)$$

According to the notation in Equation 7, it results then:

$$\mathbb{P} = proj_{\mathbf{p}}((\mathbb{A} \times \mathbb{R}^p) \cap \mathbf{f}^{-1}(\mathbb{B})) \quad (13)$$

Considering the general case where the function $\mathbf{f}$ corresponds to the composition of a rotation and a translation, the parameter vector $\mathbf{p}$ is then $\mathbf{p} = (p_1, p_2, p_3) \in \mathbb{R}^3$ with (p_1, p_2) the parameters of the 2D translation and p_3 the angle of the rotation in the 2D plane. The final function can be written as follows:

$$\mathbf{f} : \begin{cases} \mathbb{R}^2 \times \mathbb{R}^3 & \rightarrow & \mathbb{R}^2 \\ (\mathbf{x}, \mathbf{p}) & \rightarrow & \mathcal{R}(p_3) \begin{pmatrix} x_1 \\ x_2 \end{pmatrix} + \begin{pmatrix} p_1 \\ p_2 \end{pmatrix} \end{cases} \quad (14)$$

where $\mathcal{R}$ corresponds to the 2D rotation of angle p_3:

$$\mathcal{R}(p_3) = \begin{pmatrix} \cos(p_3) & -\sin(p_3) \\ \sin(p_3) & \cos(p_3) \end{pmatrix} \quad (15)$$

This general case enables to take into account the heading of the vehicle and then the visibility area with respect to the vehicle. $\mathbb{P}$ is therefore a subset of $\mathbb{R}^3$ where an inner and an outer approximation can be computed.

Consider for example a random shaped landmark $\mathbb{B}$ as depicted in Figure 3(a) where an image separator [38] [39] has been built from a binary image. Since the set $\mathbb{P}$ is a subset of $\mathbb{R}^3$, some 2D slices at fixed values are provided. At the defined heading $\theta = p_3 = 0°$, the registration map in the $(x - y)$ plane associated to the shape landmark $\mathbb{B}$ and the visibility area (given in Figure 2) is provided in Figure 3(b) according to the constraint in Equation 8. Some AUV poses with their associated visibility area are drawn to understand the solution set. At the fixed value $y = p_2 = 75m$, the solution is provided in the $(x - \theta)$ plane. The corresponding poses of the red dots are represented in Figure 3(d) where it can be noticed that all the selected poses enable to detect a part of the landmark.

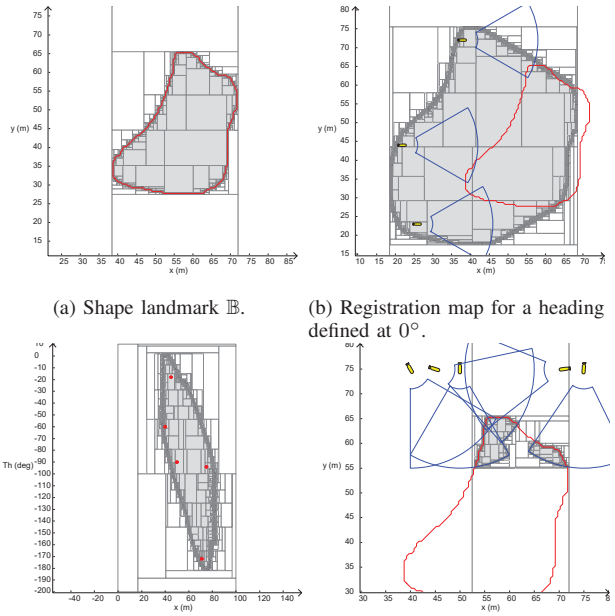

(a) Shape landmark $\mathbb{B}$.

(b) Registration map for a heading defined at $0°$.

(c) Registration map with $y = 75m$ fixed represented in the $(x - \theta)$ plane.

(d) Representation in the $(x - y)$ plane of the AUV poses defined by the red dots in the figure (c).

Fig. 3: Representation of the registration map for the FLS and the shape landmark shown by the red contour. The visibility area is shown by blue pies.

This formalization enables to compute the registration map for any landmark including punctual landmark.

IV. Motion planner

The design of the robot is low cost and therefore it is subject to high drift in position. Going straight forward from one relocation area to another is not always possible. The planning approach developed here is inspired by the open-loop strategy called preimage backchaining, originally proposed in [13], but solved here with a set-membership approach. This planning approach has been successfully used in [12] to propose a landmark based navigation where the relocation areas were only 2D disks.

A. Motion model

A robot can be described by an evolution function. Since it is assumed a 2D environment, the Dubins dynamics model is preferred for simplicity reasons. This model is defined as follows:

$$\begin{cases} \dot{x} = v \cos\theta \\ \dot{y} = v \sin\theta \\ \dot{\theta} = w \end{cases} \quad (16)$$

where $\mathbf{u} = (v, w)$ is the command of the system with v the linear speed and w the angular rate. It leads to the so-called Dubins curves [21].

Since it is assumed that the vehicle is able to follow an heading command μ_i, an holonomic motion model is proposed

through the integration of this Dubins model with $w = 0$. The trajectory of the robot is then given as follows:

$$\mathbf{f}_H : \begin{cases} \mathbb{R}^3 \times \mathbb{R} \times \mathbb{R}^2 & \rightarrow & \mathbb{R}^3 \\ (\mathbf{x}_0, t, \mathbf{p}) & \rightarrow & \begin{pmatrix} x_0 \\ y_0 \\ \theta_0 \end{pmatrix} + \begin{pmatrix} v\cos(\theta_0 + \delta_\theta)t \\ v\sin(\theta_0 + \delta\theta)t \\ \delta_\theta \end{pmatrix} \end{cases} \tag{17}$$

with $\mathbf{p} = (v, \delta_\theta)$ and v is the speed along the straight motion. δ_θ corresponds to the error on the direction θ_0.

As some relocation areas will be proposed in $\mathbb{R}^2$, the 2D version is defined as follows:

$$\mathbf{f}_{H2} : \begin{cases} \mathbb{R}^3 \times \mathbb{R} \times \mathbb{R}^2 & \rightarrow & \mathbb{R}^2 \\ (\mathbf{x}_0, t, \mathbf{p}) & \rightarrow & \begin{pmatrix} x_0 \\ y_0 \end{pmatrix} + \begin{pmatrix} v\cos(\theta_0 + \delta\theta)t \\ v\sin(\theta_0 + \delta\theta)t \end{pmatrix} \end{cases} \tag{18}$$

where the angle of arrival has been removed. Only the (x, y) coordinates are important.

According to the model in Equation 17, the pose of the robot at any time is given as follows:

$$\mathbf{x}(t) = \mathbf{f}_H(\mathbf{x}_0, t, \mathbf{p}) \tag{19}$$

where the vector $\mathbf{p}$ corresponds to the uncertain parameters.

As mentioned in Section II, the robot is able to follow uncertain heading. This uncertainty comes from the error on the compass that can be inflated to increase the guarantee. An error α_θ is then introduced. The error δ_θ on the heading measurement lies then in an interval $[-\alpha_\theta, \alpha_\theta]$. α_θ is defined at 5° in the following of this article. An uncertainty on the speed α_v is also introduced, the speed v belongs then to the following interval $v \in v_d \cdot [1 - \alpha_v, 1 + \alpha_v]$ where α_v corresponds to a rate (10%) and v_d to the desired speed (generally approximately $1m/s$). However, the speed will only influence when the landmark may be reached and not on its reachability when using directional backprojection.

The vehicle considered is then an highly manoeuvrable vehicle and is able to turn on itself to orient its head toward the desired direction. Based on this motion model, the back-projection are now defined.

B. Back projection

According to the motion model that describes uncertain linear trajectories due to uncertain directions in Equation 17, directional backprojections are defined in this article. This was also defined in [12].

Two definitions of the directional backprojection can be proposed.

1) Strong backprojection: The *strong backprojection* (**SB**) [7] defines the set of robot configurations that guarantees to reach a goal area $\mathbb{A} \subset \mathbb{R}^3$ despite the uncertainties on the motion. This corresponds to the backward reach set of a set $\mathbb{A}$ under a strategy μ. Since here the strategy is to follow a particular direction θ_d, then $\mu = \theta_d$, and the 2D backward reach set is defined as follows:

$$BACK(\mathbb{A}, \theta_d) = \{\mathbf{x} \in \mathbb{R}^3 | \forall \mathbf{p} \in [\mathbf{p}], \exists t \in \mathbb{R}^+, \\ x_3 = \theta_d \text{ and } \mathbf{f}_H(\mathbf{x}, t, \mathbf{p}) \in \mathbb{A}\} \tag{20}$$

where $\mathbf{x} = (x_1, x_2, x_3) = (x, y, \theta_d)$. Notice that actually it corresponds to a subset of $\mathbb{R}^2$ since x_3 is fixed at θ_d.

From this definition, the omnidirectional backprojection can be defined:

$$BACK_{od}(\mathbb{A}) = \{\mathbf{x} \in \mathbb{R}^3 | \forall \mathbf{p} \in [\mathbf{p}], \exists t \in \mathbb{R}^+, \mathbf{f}_H(\mathbf{x}, t, \mathbf{p}) \in \mathbb{A}\} \tag{21}$$

where 'od' means omnidirectional.

This can be reformulated as a set inversion problem:

$$BACK_{od}(\mathbb{A}) = \bigcap_{\mathbf{p} \in [\mathbf{p}]} \bigcup_{t \in \mathbb{R}^+} \mathbf{f}_H^{-1}(\mathbb{A}) \tag{22}$$

The projection notation introduced in Section III is now rewritten. Given two sets $\mathbb{X} \subset \mathbb{R}^n$ and $\mathbb{Y} \subset \mathbb{R}^p$. Considering the set $\mathbb{Z} = \mathbb{X} \times \mathbb{Y}$, the projection of a subset $\mathbb{Z}_1$ of $\mathbb{Z}$ onto $\mathbb{X}$, with respect to $\mathbb{Y}$, is defined as follows:

$$proj_{\mathbb{X}}^{\mathbb{Y}}(\mathbb{Z}_1) = \{\mathbf{x} \in \mathbb{X} | \exists \mathbf{y} \in \mathbb{Y}, (\mathbf{x}, \mathbf{y}) \in \mathbb{Z}_1\} \tag{23}$$

which leads to the following definition of the omnidirectional backprojection:

$$BACK_{od}(\mathbb{A}) = \overline{proj_{\mathbb{X}}^{\mathbb{P}}(\overline{proj_{\mathbb{X} \times \mathbb{P}}^{\mathbb{T}}(\mathbf{f}_H^{-1}(\mathbb{A}))})} \tag{24}$$

where $\mathbb{T}$ is the domain of t, $\mathbb{X}$ is the domain of $\mathbf{x}$ and $\mathbb{P}$ is the domain of the uncertain parameters $\mathbf{p}$ that is defined as follows:

$$\begin{aligned} \mathbb{P} &= [\mathbf{p}] \\ &= [v] \times [\delta_\theta] && (25) \\ &= (v_d \cdot [1 - \alpha_v, 1 + \alpha_v]) \times [-\alpha_\theta, \alpha_\theta] && (26) \end{aligned}$$

which corresponds to a box. Since the speed only influences when the landmark may be reached, the uncertainty on the speed is removed as it does not influence the reachability of the landmark. Only δ_θ is important in the reachability problem. The set $\mathbb{P}$ can then be rewritten as follows:

$$\begin{aligned} \mathbb{P} &= [\mathbf{p}] \\ &= \{v_d\} \times [\delta_\theta] && (27) \end{aligned}$$

As it may be noticed, two levels of projection are needed in Equation 22 which may be time consuming.

Under the assumption that the set $\mathbb{A}$ is connected, the omnidirectional backprojection can be defined as follows:

$$BACK_{od}(\mathbb{A}) = \bigcap_{\delta\theta \in \{-\alpha_\theta, \alpha_\theta\}} proj_{\mathbb{X}}^{\mathbb{T}}(\mathbf{f}_H^{-1}(\mathbb{A})) \tag{28}$$

where $\mathbb{X} = \mathbb{X}_1 \times \mathbb{X}_2 \times \mathbb{X}_3$ is a subset of $\mathbb{R}^3$ and corresponds to the domain of (x, y, θ) since all the trajectories are inside the bounds $\theta_d - \alpha_\theta$ and $\theta_d + \alpha_\theta$ of the uncertain direction. δ_θ is the single uncertain parameter in $\mathbf{p}$.

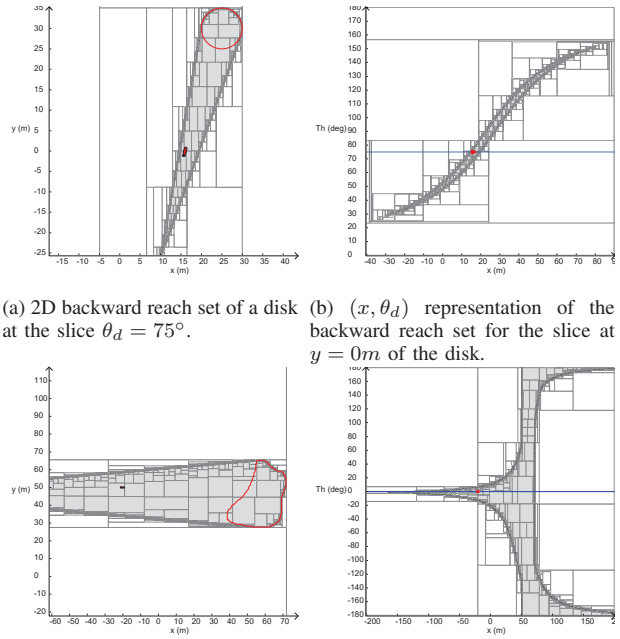

(a) 2D backward reach set of a disk at the slice $\theta_d = 75°$.

(b) (x, θ_d) representation of the backward reach set for the slice at $y = 0m$ of the disk.

(c) 2D backward reach set of a shape at the slice $\theta_d = 0°$.

(d) (x, θ_d) representation of the backward reach set for the slice at $y = 50m$ of the shape.

Fig. 4: Example of slices of the backward reach set. The blue line and the red dot in the figures on the right correspond respectively to the direction of the 2D backward reach set and the AUV pose in the figures on the left.

Similarly, the 2D backward reach set in the $(x - y)$ plane at a defined direction θ_d is defined as follows:

$$BACK(\mathbb{A}, \theta_d) = \bigcap_{\delta\theta \in \{-\alpha_\theta, \alpha_\theta\}} proj_{\mathbb{X}}^{\mathbb{T}}(\mathbf{f}_H^{-1}(\mathbb{A})) \quad (29)$$

where $\mathbb{X}$ is now the domain of x and y only ($\mathbb{X} = \mathbb{X}_1 \times \mathbb{X}_2$), and the direction θ_d is directly imposed in the function $\mathbf{f}_H$.

Notice that a level of projection has been removed from Equation 24 since it assumes a connected relocation area.

Due to the 3D representation of the omnidirectional backprojection, some slices are provided in Figure 4 for two relocation areas $\mathbb{A}$: a disk and a random shape shown by a red contour. These relocation areas are shapes in the $(x - y)$ plane then only the motion model $\mathbf{f}_{H2}$ in Equation 18 is sufficient. On the left, the directional backprojection at a defined direction is depicted. That means if the robot starts from any position inside the solution set (union of gray boxes) at the defined direction, it will reach for sure the disk or the shape despite the uncertainties on the direction. Notice that the (x, θ_d) representation for the backward reach set of the shape is actually cyclic since the fixed value $y = 50m$ crosses the shape.

2) Weak backprojection: The directional *weak backprojection* (**WB**) [7] is defined as follows:

$$\begin{aligned} WBACK(\mathbb{A}, \theta_d) = \{\mathbf{x} \in \mathbb{R}^3 | \exists \mathbf{p} \in [\mathbf{p}], \exists t \in \mathbb{R}^+ \\ x_3 = \theta_d \text{ and } \mathbf{f}_H(\mathbf{x}, t, \mathbf{p}) \in \mathbb{A}\} \end{aligned} \quad (30)$$

and the omnidirectional weak backprojection:

$$\begin{aligned} WBACK_{od}(\mathbb{A}) = \{\mathbf{x} \in \mathbb{R}^3 | \exists \mathbf{p} \in [\mathbf{p}], \exists t \in \mathbb{R}^+, \\ \mathbf{f}_H(\mathbf{x}, t, \mathbf{p}) \in \mathbb{A}\} \end{aligned} \quad (31)$$

Notice the difference with the strong backprojection that guarantees all the trajectories will cross $\mathbb{A}$ contrary to the weak backprojection that proves at least one uncertain direction crosses $\mathbb{A}$ due to the uncertain parameter δ_θ.

According to the definition of the projection, the directional weak backprojection can be computed as follows:

$$WBACK(\mathbb{A}, \theta_d) = proj_{\mathbb{X}}^{\mathbb{P} \times \mathbb{T}}(\mathbf{f}_H^{-1}(\mathbb{A})) \quad (32)$$

where $\mathbb{X} = \mathbb{X}_1 \times \mathbb{X}_2$ and the direction θ_d is directly injected in the function $\mathbf{f}_H$.

Similarly, it can be defined:

$$WBACK_{od}(\mathbb{A}) = proj_{\mathbb{X}}^{\mathbb{P} \times \mathbb{T}}(\mathbf{f}_H^{-1}(\mathbb{A})) \quad (33)$$

where $\mathbb{X} = \mathbb{X}_1 \times \mathbb{X}_2 \times \mathbb{X}_3$.

Some examples will be provided in the next subsection with forbidden areas.

C. Back projection with forbidden areas

Due to the assumption of indistinguishable landmarks (or relocation areas), these landmarks have to be taken into account in the computation of the backward reach set of the relocation area associated to a landmark. Define as $\mathbb{O}$ ("O" like Obstacles), the set of connected forbidden areas $\mathbb{O}_i \subset \mathbb{R}^3$ which is given as follows:

$$\mathbb{O} = \bigcup_{i \in \{0,..,N\}} \mathbb{O}_i \quad (34)$$

When the robot has to reach a relocation area $\mathbb{A}$, it does not have to cross another relocation area $\mathbb{O}_i$ due to the possible wrong data association. These forbidden areas may be obstacles too, and can be taken into account for obstacles avoidance.

The omnidirectional backward reachability of a set $\mathbb{A} \subset \mathbb{R}^3$ considering forbidden areas $\mathbb{O}$ is given as follows:

$$\begin{aligned} BACK_{od}^{\mathbb{O}}(\mathbb{A}) &= \{\mathbf{x} \in \mathbb{R}^3 | \forall \delta_\theta \in [-\alpha_\theta, \alpha_\theta], \exists t \in \mathbb{R}^+, \\ &\quad \mathbf{f}_H(\mathbf{x}, t, \mathbf{p}) \in \mathbb{A} \text{ and } \forall \delta_\theta \in [\alpha_\theta, \alpha_\theta], \\ &\quad \forall t \in \mathbb{R}^+, \mathbf{f}_H(\mathbf{x}, t, \mathbf{p}) \notin \mathbb{O}\} \\ &= BACK_{od}(\mathbb{A}) \cap \overline{WBACK_{od}(\mathbb{O})} \end{aligned} \quad (35)$$

Due to the 3D representation of the omnidirectional backprojection taking into accout another relocation areas, some slices are provided in Figure 5 where the goal set to reach is the disk $\mathbb{A}$ and the forbidden areas are $\mathbb{O}_1$ and $\mathbb{O}_2$

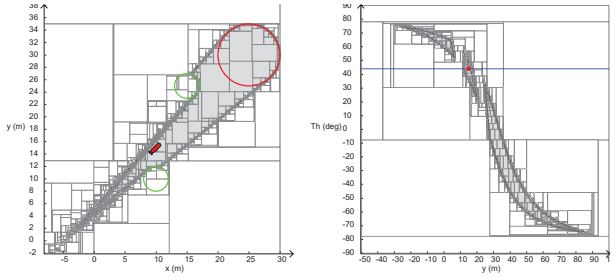

(a) 2D backward reach set of a disk at the slice $\theta_d = 45°$.

(b) (y, θ_d) representation of the backward reach set for the slice at $x = 10m$.

Fig. 5: Example of slices of the backward reach set taking into account forbidden areas. The blue line and the red dot in the figure (b) correspond respectively to the direction of the 2D backward reach set and the AUV pose in the figure (a).

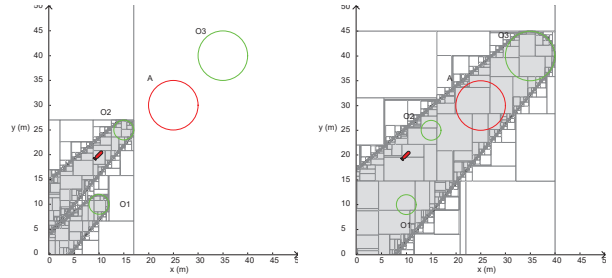

(a) 2D weak backprojection $WBACK(\mathbb{O}_1 \cup \mathbb{O}_2, \theta_d = 45°)$.

(b) 2D weak backprojection $WBACK(\mathbb{O}_1 \cup \mathbb{O}_2 \cup \mathbb{O}_3, \theta_d = 45°)$.

Fig. 6: Weak backprojection of forbidden areas at the defined direction $\theta_d = 45°$.

(disks too).

However, Equation 35 is not always true especially when a forbidden area lies behind the goal area as shown in Figure 6. At the defined direction $\theta_d = 45°$, the 2D weak backprojection considering only $\mathbb{O}_1$ and $\mathbb{O}_2$ as forbidden areas is shown in Figure 6(a) which leads to the result in Figure 5(a) according to Equation 35. If a third relocation area $\mathbb{O}_3$ is considered with $\mathbb{O}_1$ and $\mathbb{O}_2$, the 2D weak backprojection, depicted in Figure 6(b), covers the 2D backprojection (strong) of the goal area leading to an empty result. This third set $\mathbb{O}_3$ lies behind the goal area at the direction $\theta_d = 45°$. To generate the backprojection of a goal area in presence of another relocation areas that may create ambiguity, it has to be handled carefully by removing $\mathbb{O}_3$ in the example proposed.

D. Path finding

A method to compute omnidirectional backprojection of relocation areas, even in presence of ambiguous relocation areas, has been presented. The different relocation areas are nodes of hyper-graph. Contrary to the 2D example of goal area presented earlier, the relocation areas are now the registration maps introduced in Section III which are subsets of $\mathbb{R}^3$. The motion function is then $\mathbf{f}_H$ since the angle of arrival has an influence due the limited FOV of the sensor. The creation of the links has now to be established to create the edges in the graph.

1) Connection between registration maps: Consider respectively two registration maps $\mathbb{A}$ and $\mathbb{B}$ associated to two landmarks A and B computed according to Equation 8 in Section III based on the visibility area of the sensor. Assume that the departure landmark is A and the landmark to reach is B (goal landmark). Due to the ability of the robot to turn on itself and orient its head at the desired direction based on the heading measurement provided by the compass, two methods of departure area may be envisaged.

The first method consists in starting the robot motion at a desired direction only if it can detect the departure landmark. This solution enables to have a reliable position estimation of the robot at the beginning of the motion to reach the goal landmark since it can detect this first geolocalized landmark. A link between A and B despite the uncertainties on the motion is computed as follows:

$$\mathbb{X}_{\mathbb{A}\rightarrow\mathbb{B}} = \{\mathbf{x} \in \mathbb{R}^3 | BACK_{od}(\mathbb{B}) \cap \mathbb{A} \neq \emptyset\} \tag{36}$$

It corresponds to the set of robot configurations able to detect the landmark A and that are guaranteed to detect the landmark B at certain time despite the uncertainty on the direction $\delta_\theta \in [-\alpha_\theta, \alpha_\theta]$ along the motion. In other words, all the posible trajectories having an initial pose in $\mathbb{X}_{\mathbb{A}\rightarrow\mathbb{B}}$ cross the registration map $\mathbb{B}$ associated to B enhancing its detection. The direction of the arrow indicates the registration map to reach. Based on the SIVIA algorithm, if the set $\mathbb{X}_{\mathbb{A}\rightarrow\mathbb{B}}$ is not empty, there is at least one pose that can detect A and can detect after the uncertain motion the landmark B. At a defined direction θ_d, the set of robot positions can be computed as follows:

$$\mathbb{P}_{\mathbb{A}\rightarrow\mathbb{B}}(\theta_d) = \{(x_1, x_2) \in \mathbb{R}^2 | BACK(\mathbb{B}, \theta_d) \cap \mathbb{A}(\theta_d) \neq \emptyset\} \tag{37}$$

where $\mathbb{A}(\theta_d)$ corresponds to the slice of the registration map at the defined heading θ_d.

Due to the ability to turn on itself, the second method consists in detecting the departure landmark and then orient the head at a desired direction to reach the goal landmark. An uncertainty can be added to the position after the rotation but it is assumed here that this uncertainty is null. Only the range of detection of the sensor is important now to compute the registration map which can be computed by removing the heading constraint of the vehicle and considering an aperture angle of 360° (range only sensor). The visibility area is then simply a ring and only the translation parameters have to be computed to generate the registration map. This registration map corresponds to:

$$\mathbb{A}_{2D} = proj^{\mathbb{X}_3}_{\mathbb{X}_1\times\mathbb{X}_2}(\mathbb{A}) \tag{38}$$

which is simply the projection on the ground (in the $(x - y)$ plane) of the registration map $\mathbb{A}$.

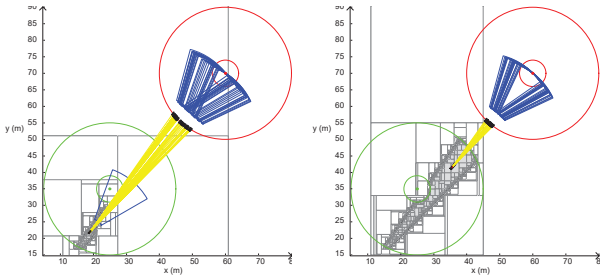

(a) Departure position that can see the landmark. (b) Departure after rotation on itself.

Fig. 7: Two methods of departure positions to reach a goal punctual landmark in red at the defined direction $\theta_d = 50°$.

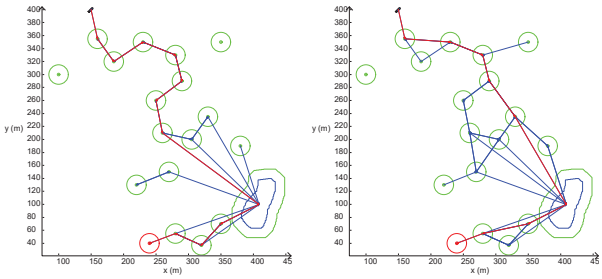

(a) Starting poses using the first method. (b) Starting poses using the second method.

Fig. 8: Strategy found in red and links in blue between registration maps. The departure position is at the top (blue AUV) and the target at the bottom (red punctual target). Circles are minimal and maximal ranges of detection of the punctual landmarks. A shape landmark is present in blue with the visibility at R_{max} in green.

The connection can be reformulated now as follows:

$$\mathbb{X}_{\mathbb{A}\to\mathbb{B}} = \{\mathbf{x} \in \mathbb{R}^3 | BACK_{od}(\mathbb{B}) \cap (\mathbb{A}_{2D} \times \mathbb{R}) \neq \emptyset\} \quad (39)$$

where $\mathbb{R}$ has to be added for the correspondance of dimension. The angle of departure has no influence.

The set of departure positions can then be simply computed at a defined direction θ_d as follows:

$$\mathbb{P}_{\mathbb{A}\to\mathbb{B}}(\theta_d) = \{(x_1, x_2) \in \mathbb{R}^2 | BACK(\mathbb{B}, \theta_d) \cap \mathbb{A}_{2D} \neq \emptyset\} \quad (40)$$

An example is provided in Figure 7 where the departure landmark is the punctual green landmark and the goal landmark is the red punctual landmark. The circles are the minimal (R_{min}) and maximal (R_{max}) ranges of detection. At the defined direction $\theta_d = 50°$, the set of departure positions using the first method is given in Figure 7(a) and using the second method is given in Figure 7(b). One position (blue AUV) is selected in the different solution sets from where the uncertain trajectories are generated due to the uncertainty on the direction in yellow. The poses and the visibility area are drawn in blue when it detects the red punctual goal landmark. All the trajectories can detect the goal landmark and none are lost.

2) Graph creation and optimization: A backward graph search is performed starting from the target registration map. Only the $K-$nearest neighbours are considered for each registration map to reduce the complexity of the graph construction. When the set linking two registration maps in Equation 36 or in Equation 39, depending on the strategy of the planner, is not empty then an edge may be created. However, as mentioned in Section IV-C about forbidden areas, ambiguous local landmarks (if some exists) have to be taken into account to avoid wrong data association due to the indistinguishable property of the landmarks. This can be realized by considering the omnidirectional backprojection taking into account these ambiguous landmarks as in Equation 35. A link can then be created. Moreover, a graph optimization based on A* [40] algorithm is realized to propose an optimal path which is here simply based on the distance between the centroids of the shapes. The path found will provide a minimal path length.

V. Experiments

A simple example based only on simulation is now provided as experiments. Consider a sensor that can detect between $R_{min} = 2m$ and $R_{max} = 15m$ and has an half aperture angle $\theta_3 = 20°$. The error on the compass is fixed at $5°$. An environment is proposed in Figure 8 where many punctual landmarks (green dot) are present and a shape landmark in blue. A punctual red target lies in the bottom of the figure and the initial position of the robot, represented by the blue AUV, is at the top. The visibility at R_{min} and R_{max} of the punctual landmarks and the target is shown by circles. The visibility at R_{max} of the shape is drawn by the green contour. These areas correspond to the projection on the ground (in the $(x-y)$ plane) of the registration maps associated to the different landmark. It represents $\mathbb{A}_{2D}$.

The graph construction using the two strategies for the departure position is depicted in Figure 8 where the blue links are valid edges and the final strategy found is represented by the red arrows. As it may be noticed the strategy is not the same. Indeed, using the first method, the robot can only start its motion from a position that is able to detect the landmark contrary to the second method that enables the robot to turn on itself before leaving the departure registration map.

Some directions are selected in the solution sets for the two strategies found to propose the set of departure positions taking into account the different local ambiguous landmarks in Figure 9(a) and (c). Some departure AUV positions are then selected in the different departure areas shown by red AUVs. The path execution is then represented in Figure 9(b) and (d) for these two strategies. The uncertain trajectories due to the uncertain directions are represented by yellow lines starting from the red AUV departure positions. When it detects the landmark, the visibility area is represented by a blue pie for the blue AUV corresponding pose. Magenta lines correspond to the relocation process to join the departure

position. This correspond to the visually guided navigation where it is assumed that a low level controller is able to perform this task. All the trajectories are able to detect the considered landmark each times without ambiguity and are able to reach the target at the bottom.

VI. Conclusion and Future Works

In this article we present a motion planner that guarantees the reachability of a target by a low cost AUV equipped with an exteroceptive sensor in the underwater context. Due to the drift in position and a potential far diving position, going straight forward to the target is rarely the solution for an AUV with a poor navigation. The alternative solution proposed is to use an *an priori* map of the environment composed of static landmarks that are *a priori* detectable by the exteroceptive sensor under the strategy of navigation such as the altitude. Based on the location of the different landmarks in the environment, a registration map is firstly computed depending on the visibility area of the sensor embedded in the robot. This map indicates the set of robot configurations able to detect a landmark. This set is called relocation area and enables to reduce the uncertainty of the robot pose by detecting the considered landmark. Secondly, the motion planner inspired by the works [13] [12] [41] based on the concept of preimage backchaining, proposes a sequence of action to realize that guarantees the revisit of the target by revisiting intermediate landmarks. The preimage backchaining is solved in a set membership manner by taking into account the drift of the robot modelled by uncertain trajectories. The preimage backchaining relies on backprojections that are defined as backward reach set of a registration map according to the uncertain motion model. By proving links between the relocation areas despite uncertainties on the motion, the robot is then able to navigate safely between the relocation areas, and relocate thanks to the landmark position by making an exteroceptive measurement. Relocation areas consitute then the nodes of a hyper graph. Handled by a graph search algorithm minimizing a cost function, it starts from the target relocation area(s) and computes the successive backprojection until the initial position of the robot is included in a backprojection. It alternates phases of motion command and relocation process in the different relocation areas to reduce the uncertainty of the robot. Compared to other probabilistic approaches [26], the set membership method based on the notion of separators and projectors [30] [39] provides the guarantee information if the uncertain parameters remain in their bounded intervals.

Future works will focus on the fact that a landmark may not be detected during the path execution. To avoid being lost, a strategy based on SLAM (Simultaneous Localization And Mapping) may be envisaged to register the new map to the *a priori* map, and then be relocated relatively to the first landmarks map. Another improvement would be to consider an uncertainly defined map such as uncertainly located punctual landmarks. The registration maps concept has then to be

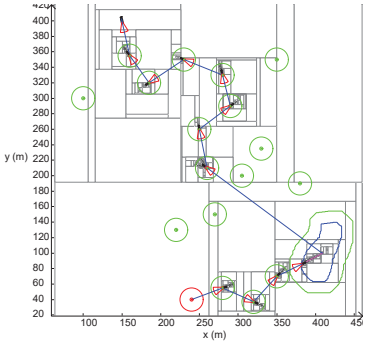

(a) Departure positions with the first method.

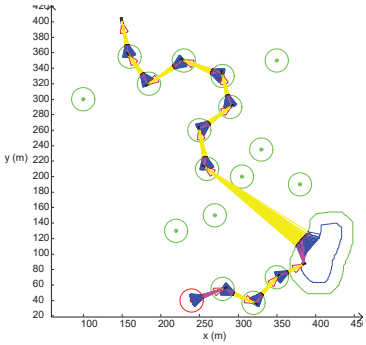

(b) Trajectories simulation for the strategy using the first method. Yellow lines are uncertain trajectories and magenta relocation processes. Blue pies are visibility areas when detecting the landmark.

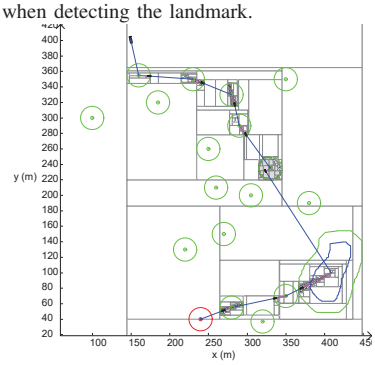

(c) Departure positions with the second method.

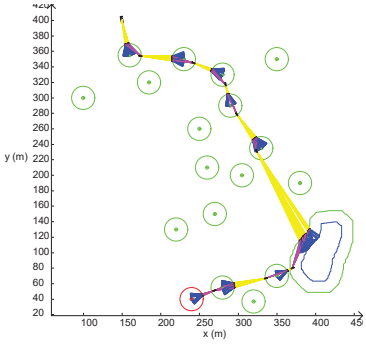

(d) Trajectories simulation for the strategy using the second method.

Fig. 9: Path execution of the two strategies according to the two departure methods.

adapted to consider these uncertain definition of the landmarks. Moreover some real experiments should be conducted to validate the principle.

REFERENCES

[1] D. Gibbins and J. Adams. Shipwrecks and maritime archaeology. *World Archaeology*, 32(3):279–291, 2001.

[2] R. Eustice, H. Singh, J. J. Leonard, M. R. Walter, and R. Ballard. Visually navigating the rms titanic with slam information filters. In *Robotics: Science and Systems*, volume 2005, pages 57–64, 2005.

[3] B. Nguyen, M. J. Bays, A. Shende, and D. J. Stilwell. An approach to subsea survey for safe naval transit. In *OCEANS 2011*, pages 1–6. IEEE, 2011.

[4] K. Vickery. Acoustic positioning systems. a practical overview of current systems. In *Autonomous Underwater Vehicles, 1998. AUV'98. Proceedings of the 1998 Workshop on*, pages 5–17. IEEE, 1998.

[5] M. F. Fallon, J. Folkesson, H. McClelland, and J. J. Leonard. Relocating underwater features autonomously using sonar-based slam. *IEEE Journal of Oceanic Engineering*, 38(3):500–513, 2013.

[6] N. R. Gracias, S. Van Der Zwaan, A. Bernardino, and J. Santos-Victor. Mosaic-based navigation for autonomous underwater vehicles. *IEEE Journal of Oceanic Engineering*, 28(4):609–624, 2003.

[7] S. M. LaValle. *Planning algorithms*. Cambridge university press, 2006.

[8] J. C. Latombe. *Robot Motion Planning*. Springer Science & Business Media, 1991.

[9] M. Couillard, J. Fawcett, and M. Davison. Optimizing constrained search patterns for remote mine-hunting vehicles. *IEEE Journal of Oceanic Engineering*, 37(1):75–84, 2012.

[10] H. Takeda and J. C. Latombe. Sensory uncertainty field for mobile robot navigation. In *Robotics and Automation, 1992. Proceedings., 1992 IEEE International Conference on*, pages 2465–2472. IEEE, 1992.

[11] N. Roy, W. Burgard, D. Fox, and S. Thrun. Coastal navigation-mobile robot navigation with uncertainty in dynamic environments. In *Robotics and Automation, 1999. Proceedings. 1999 IEEE International Conference on*, volume 1, pages 35–40. IEEE, 1999.

[12] A. Lazanas and J. C. Latombe. Motion planning with uncertainty: a landmark approach. *Artificial intelligence*, 76(1-2):287–317, 1995.

[13] Tomas Lozano-Perez, Matthew T Mason, and Russell H Taylor. Automatic synthesis of fine-motion strategies for robots. *The International Journal of Robotics Research*, 3(1):3–24, 1984.

[14] B. Bouilly, T. Simeon, and R. Alami. A numerical technique for planning motion strategies of a mobile robot in presence of uncertainty. In *Robotics and Automation, 1995. Proceedings., 1995 IEEE International Conference on*, volume 2, pages 1327–1332. IEEE, 1995.

[15] J. P. Gonzalez and A. Stentz. Planning with uncertainty in position using high-resolution maps. In *Robotics and Automation, 2007 IEEE International Conference on*, pages 1015–1022. IEEE, 2007.

[16] A. Censi, D. Calisi, A. De Luca, and G. Oriolo. A bayesian framework for optimal motion planning with uncertainty. In *Robotics and Automation, 2008. ICRA 2008. IEEE International Conference on*, pages 1798–1805. IEEE, 2008.

[17] Th. Fraichard and R. Mermond. Integrating uncertainty and landmarks in path planning for car-like robots. In *Proc. IFAC Symp. on Intelligent Autonomous Vehicles March*, volume 25, page 27, 1998.

[18] T. Fraichard and R. Mermond. Path planning with uncertainty for car-like robots. In *ICRA*, pages 27–32, 1998.

[19] A. Lambert and Th. Fraichard. Landmark-based safe path planning for car-like robots. In *Robotics and Automation, 2000. Proceedings. ICRA'00. IEEE International Conference on*, volume 3, pages 2046–2051. IEEE, 2000.

[20] P. Švestka and M. H. Overmars. Probabilistic path planning. In *Robot motion planning and control*, pages 255–304. Springer, 1998.

[21] L. E. Dubins. On curves of minimal length with a constraint on average curvature, and with prescribed initial and terminal positions and tangents. *American Journal of mathematics*, 79(3):497–516, 1957.

[22] R. Pepy, M. Kieffer, and E. Walter. Reliable robust path planning. *International Journal of Applied Mathematics and Computer Science*, 19(3):413–424, 2009.

[23] R. Pepy and A. Lambert. Safe path planning in an uncertain-configuration space using rrt. In *Intelligent Robots and Systems, 2006 IEEE/RSJ International Conference on*, pages 5376–5381. IEEE, 2006.

[24] A. Lambert and N. Le Fort-Piat. Safe task planning integrating uncertainties and local maps federations. *The International Journal of Robotics Research*, 19(6):597–611, 2000.

[25] S. Prentice and N. Roy. The belief roadmap: Efficient planning in belief space by factoring the covariance. *The International Journal of Robotics Research*, 28(11-12):1448–1465, 2009.

[26] S. Thrun. Probabilistic algorithms in robotics. *Ai Magazine*, 21(4):93, 2000.

[27] S. Saripalli, J. F. Montgomery, and G. S. Sukhatme. Visually guided landing of an unmanned aerial vehicle. *IEEE transactions on robotics and automation*, 19(3):371–380, 2003.

[28] B. Desrochers and L. Jaulin. Computing a guaranteed approximation of the zone explored by a robot. *IEEE Transactions on Automatic Control*, 62(1):425–430, 2017.

[29] C. Pradalier and S. Sekhavat. " localization space": a framework for localization and planning, for systems using a sensor/landmarks module. 2002.

[30] Luc Jaulin and Benoît Desrochers. Introduction to the algebra of separators with application to path planning. *Engineering Applications of Artificial Intelligence*, 33:141–147, 2014.

[31] L. Jaulin and E. Walter. Set inversion via interval analysis for nonlinear bounded-error estimation. *Automatica*, 29(4):1053–1064, 1993.

[32] R. E. Moore. *Methods and applications of interval analysis*, volume 2. Siam, 1979.

[33] B. Desrochers and L. Jaulin. A minimal contractor for the polar equation: Application to robot localization. *Engineering Applications of Artificial Intelligence*, 55:83–92, 2016.

[34] B. Zitova and J. Flusser. Image registration methods: a survey. *Image and vision computing*, 21(11):977–1000, 2003.

[35] P. J. Besl and N. D. McKay. A method for registration of 3-d shapes. *IEEE Transactions on Pattern Analysis and Machine Intelligence*, 14(2):239–256, 1992.

[36] C. Chailloux, J. M. Le Caillec, D. Gueriot, and B. Zerr. Intensity-based block matching algorithm for mosaicing sonar images. *IEEE Journal of Oceanic Engineering*, 36(4):627–645, 2011.

[37] B. Desrochers and L. Jaulin. Minkowski operations of sets with application to robot localization. *arXiv preprint arXiv:1704.03103*, 2017.

[38] J. Sliwka. *Using set membership methods for robust underwater robot localization*. PhD thesis, Ensta Bretagne, 2011.

[39] B. Desrochers. *SLAM in unstructured environments; a set-membership approach*. PhD thesis, Brest, 2018.

[40] P. E. Hart, N. J. Nilsson, and B. Raphael. A formal basis for the heuristic determination of minimum cost paths. *IEEE transactions on Systems Science and Cybernetics*, 4(2):100–107, 1968.

[41] M. Erdmann. Using backprojections for fine motion planning with uncertainty. *The International Journal of Robotics Research*, 5(1):19–45, 1986.